Modeling arsenic (V) removal from water by micellar enhanced ultrafiltration in the presence of competing anions

Ming Chen[a,b], Karen Shafer-Peltier[b], Stephen J. Randtke[a], Edward Peltier[a,]*

[a.] *Department of Civil, Environmental and Architectural Engineering, University of Kansas, KS 66045*

[b.] *Tertiary Oil Recovery Program, University of Kansas, KS 66045*

[*]*Corresponding author:* epeltier@ku.edu

Abstract: With increasing arsenic (As) contamination incidents reported around the world, better processes for As removal from industrial wastewater and other contaminated waters are required to protect drinking water sources. Complexation of As with cetylpyridinium chloride (CPC) cationic surfactant micelles, coupled with ultrafiltration (UF), has the potential to improve As removal, but competition from other anions could be a limiting factor. Using a binary-system ion-exchange model, the selectivity coefficients for binding of the monovalent and divalent forms of arsenate (As (V)) to cationic cetylpyridinium (CP^+) micelles, relative to Cl^-, were determined to be 0.55 for $H_2AsO_4^-$ and 0.047 mol L^{-1} for $HAsO_4^{2-}$, respectively. The affinity sequence for binding of commonly occurring monovalent anions by CP^+ micelles was found to be $NO_3^- > Cl^- > HCO_3^- > H_2AsO_4^-$, and for divalent anions, $SO_4^{2-} > HAsO_4^{2-}$. Distribution of As (V) between the micellar and aqueous phases was explored using ion exchange isotherms, with higher pH and lower concentrations of competing anions increasing rejection of As (V) across UF membranes. A model accounting for these effects, based on mass balances across UF membranes and selectivity coefficients for binding of anions to the CP^+ micelles, was used to predict As (V) removal during micellar-enhanced ultrafiltration (MEUF) of mixtures of competing anions. Model predictions agreed well with experiment results for both artificial and spiked natural river water samples. Arsenic ($\approx$ 0.1 mM) removals of 91% and 84% were achieved from artificial waters and spiked natural river waters, respectively, by adding 20 mM CPC prior to UF.

Keywords: Surfactant micelles; Arsenic; Ion exchange; Micellar enhanced ultrafiltration (MEUF); Prediction model

1 Introduction

Notable contamination of water with arsenic (As) has been reported in many countries, including Bangladesh, Chile, Argentina and China (Jiang et al., 2015; Singh et al., 2015; McArthur et al., 2016; Schwanck et al., 2016). Arsenic is a naturally occurring element that can be released into solution from weathering and dissolution of minerals in rocks and soil (Cullen and Reimer, 1989; Garelick et al., 2009). A number of anthropogenic activities can also contribute to As pollution in water, including petroleum refining, mining, wood preservation, and various agricultural and industrial activities (Chilvers and Peterson, 1987; Savery et al., 2014; Liu et al., 2015). Arsenic has high toxicity, carcinogenicity, and potential to bio-accumulate (Jain and Ali, 2000; Han et al., 2004; Bräuner et al., 2014). U.S. EPA has therefore set a maximum allowable As level in drinking water of 10 $\mu g\ L^{-1}$ (EPA, 2001). Effective treatment processes to separate As from contaminated wastewaters and runoff can help to reduce As exposure and maintain the quality of drinking water sources.

Arsenic bioaccumulation, toxicity and mobility in the environment are strongly affected by chemical speciation and spatial distribution (Han et al., 2004). Arsenate (As (V)) is generally the dominant aqueous inorganic arsenic species under oxidizing conditions, and is typically found in shallow groundwater and surface waters under aerobic conditions (Welch et al., 2000). Arsenite (As (III)) is the dominant species under reducing (anoxic) conditions commonly found in deeper groundwater (Cullen and Reimer, 1989; Welch et al., 2000; Sorg et al., 2014). Arsenite has a higher toxicity and is more difficult to eliminate from water than As (V) (EPA, 2001), but is easily converted to As (V) by oxidation (Bissen and Frimmel, 2003; Dodd et al., 2006; Zhou et al., 2013). Treatment of surface waters thus typically focuses on As (V). Arsenic acid is a triprotic acid, with dissociation reactions and constants as shown in **eqs 1-3** (Gecol et al., 2004; Rivas et al., 2007).

(A pC-pH diagram and a predominance area diagram for arsenic acid are shown in **Figures 1S and 2S**, respectively, in the **Supporting Information**.)

$$H_3AsO_4 \overset{K_{a1}}{\Longleftrightarrow} H^+ + H_2AsO_4^-, pK_{a1} = 2.22 \quad (1)$$

$$H_2AsO_4^- \overset{K_{a2}}{\Longleftrightarrow} H^+ + HAsO_4^{2-}, pK_{a2} = 6.98 \quad (2)$$

$$HAsO_4^{2-} \overset{K_{a3}}{\Longleftrightarrow} H^+ + AsO_4^{3-}, pK_{a3} = 11.4 \quad (3)$$

$H_2AsO_4^-$ and $HAsO_4^{2-}$ are the dominant arsenate species in the pH range of 6 - 9, which is typical of surface waters and groundwaters. Therefore, treatment technologies for removing As from solution usually target one or both of these species. Conventional technologies used to remove arsenic from water include adsorption (Hong et al., 2014), coagulation or precipitation (Cui et al., 2015), ion exchange (Elton et al., 2013; Dominguez-Ramos et al., 2014), and membrane separation (Mondal et al., 2014; Molinari and Argurio, 2017). Removal performance for most processes is strongly pH dependent because of pH effects on both arsenate speciation and exchange, sorption, and precipitation reactions. Membrane separation processes such as nanofiltration and reverse osmosis can remove up to 90% to 95% of arsenic from water; however, these processes require high operating pressures and high energy inputs (EPA, 2000; Ning, 2002; Mondal et al., 2014). Ultrafiltration (UF) operates at lower pressures, requiring less energy, but it does not remove low molecular weight dissolved constituents unless they are first incorporated into larger particles or complexes. Micellar enhanced ultrafiltration (MEUF), in which ionic surfactant micelles are used to complex dissolved aqueous pollutants, increasing their size and thus their removal by UF, has been studied extensively due to its high separation efficiency and low energy requirement (Schwarze et al., 2015; Huang et al., 2017; Schwarze, 2017; Huang et al., 2018). Ionic surfactant micelles form when the concentration of surfactant

75 exceeds the critical micelle concentration (CMC). These micelles act as nano-sized ion
76 exchangers and, consequently, ionic pollutants associated with them can be removed when the
77 micelles are rejected by a UF membrane.

78 Previous studies (Beolchini et al., 2006, 2007; Iqbal et al., 2007; Jafari et al., 2017) on arsenic
79 removal by MEUF have focused on As (V) removal as a function of surfactant type and material,
80 surfactant concentration, operating conditions such as trans-membrane pressure, and
81 membrane molecular weight cut-off (MWCO). Greater than 90% removal of As (V) (at initial
82 concentrations from 29 μg L^{-1} to 10 mg L^{-1}) was observed in these studies using
83 cetyltrimethylammonium bromide (CTAB) and cetylpyridinium chloride (CPC) during MEUF.
84 Some researchers have considered the influence of competing anions on As (V) removal (Ergican
85 et al., 2005; Iqbal et al., 2007; Ergican and Gecol, 2008), however, these results were achieved in
86 synthetic samples or groundwater, and there is a general lack of research focusing on As (V)
87 removal from complex ionic mixtures and the effects of pH. In wastewater and runoff, arsenic
88 speciation will be governed by pH, while competition from commonly occurring anions such as
89 HCO_3^-, Cl^-, NO_3^-, and SO_4^{2-} may adversely affect removal of target anions (Tang et al., 2015; Xie et
90 al., 2015).

91 The objective of this study was to model As (V) removal from water by MEUF, taking into
92 consideration the effects of pH and competing anions. To accomplish this, experiments were
93 conducted using an MEUF system with cationic micelles composed of cetylpyridinium (CP^+) ions.
94 CPC was chosen because it was previously found to achieve higher removal of anionic
95 constituents than other typical cationic surfactants (Iqbal et al., 2007). The results of
96 experiments on binary mixtures of anions were used to calculate selectivity coefficients for
97 binding of the ions of interest to the CP^+ micelles. These coefficients were then incorporated

into a simplified model for anion distribution in micellar solutions (Chen and Jafvert, 2017) that was used to predict removal of monovalent and divalent As (V) ions by MEUF from synthetic solutions and natural waters containing mixtures of competing anions, i.e., HCO_3^-, Cl^-, NO_3^-, and SO_4^{2-}.

2 Materials and methods

2.1 Materials

Cetylpyridinium chloride monohydrate (CPC, 99.0-102.0%) purchased from Sigma-Aldrich, with a CMC of 1.08 mM (Lee et al., 2005) in pure water at room temperature, was used as the cationic surfactant. Analytical grade sodium arsenate dibasic heptahydrate ($Na_2HAsO_4{\cdot}7H_2O$) supplied by Aldrich Chemical was used as the arsenate source. To determine selectivity coefficients, solutions containing predominantly $H_2AsO_4^-$ or $HAsO_4^{2-}$ were prepared by adjusting pH to 4.5 or 9.0, respectively, after CPC addition, by dropwise addition of 0.1 M HCl or NaOH, respectively. Solutions of other anions, including Cl^-, HCO_3^-, NO_3^-, and SO_4^{2-}, were prepared from their respective sodium salts. These and all other chemical reagents were ACS reagent grade. Ultrapure water (18.2 MΩ cm^{-1}, Milli-Q Direct 8 system) was used in all experiments.

The natural water sample used in this study was collected from the Kansas River at Lawrence, KS and filtered through a 0.45 µm filter to remove suspended solids. The anionic composition of the water sample is provided in **Table 1S in the Supporting Information**. The concentrations of Cl^- and SO_4^{2-} are relatively high, perhaps in part because the collection site was close to the discharge point of a wastewater treatment plant. Subsamples were spiked with 0.12 mM Na_2HAsO_4 (As ≈ 9 mg L^{-1}).

2.2 Ultrafiltration process

A stirred dead-end ultrafiltration cell (Amicon, USA, model 8200) and cellulose membranes (YM10, Amicon, USA) with diameter of 62 mm and effective area of 28.7 cm^2 were used to separate the aqueous phase from the micellar phase. The molecular weight cut-off (MWCO) of the membranes was 10 kDa. All experiments were conducted at room temperature and at a pressure of 30 psi. Anions and CP^+ micelles were contacted for 30 min before ultrafiltration. Sample pH was adjusted by adding HCl or NaOH and measured using a pH meter (Fisher Accumet AB15) with a glass pH electrode (Fisher Accumet Cat. #13-620-223A).

The total volume of the experimental water samples was 100 mL. Subsamples of each solution collected after CPC addition, but before filtration, and the first 10 mL of permeate were analyzed to determine the total concentration of each anion initially present and the concentrations present following MEUF, respectively.

The rejection fraction (or removal) of As, *R*, is defined by **eq 4**.

$$R = 1 - \frac{[As]_{aq}}{[As]_{total}} \qquad (4)$$

where $[As]_{aq}$ and $[As]_{total}$ refer to As concentrations in the permeate (aqueous concentration) and the feed solution (total concentration), respectively.

2.3 Analytical procedures

Arsenic concentrations were determined using an inductively coupled plasma-optical emission spectrometer (ICP-OES, PerkinElmer, Optima 2000 DV). Samples were acidified with 2% (by volume) HNO_3 (Fisher Scientific PN A509) prior to analysis. Triplicate ICP analyses were performed for each sample, and measurements accepted if all results were within 10% of the averaged value. CPC concentrations were determined using a UV-Visible spectrophotometer (Shimadzu, UV-1650PC) at a wavelength of 259 nm. (The spectrum and standard curve are shown in **Figures 3S and 4S** in the **Supporting Information**.) Aqueous concentrations of Cl^-, NO_3^-

and SO_4^{2-} were determined using ion chromatography (IC, Dionex ICS 2000). A Dionex IonPac AS18 column was used to separate anions using a mobile phase of 30 mM KOH with a flow rate of 1.0 mL/min. HCO_3^- concentrations were determined by titration (APHA et al., 2012).

2.4 Selectivity coefficients for ion exchange on micelles

Ionic surfactant micelles can be treated as nano-sized colloidal particles with electrical charges, i.e., ion exchangers, and the association of counterions with micelles can be described using the triple-layer model (Rathman and Scamehorn, 1984; Lin and Jafvert, 2000) shown in **Figure 1**. The first layer is the surfactant molecules, and the second layer (commonly referred to as the Stern layer) consists of hydrated counterions tightly associated with (bound to) the micellar surface. Most ionic sites on the micellar surface are occupied by the associated counterions. The third layer is the diffuse layer between the Stern layer and the bulk solution phase, in which both the electrical potential and the concentrations of counterions drop off as a function of distance from the Stern layer. The model is in essence a two-phase model that considers all counterions in the micellar solution to exist either as bound ions (in the Stern layer) or unbound free ions (in the diffuse layer and in bulk solution).

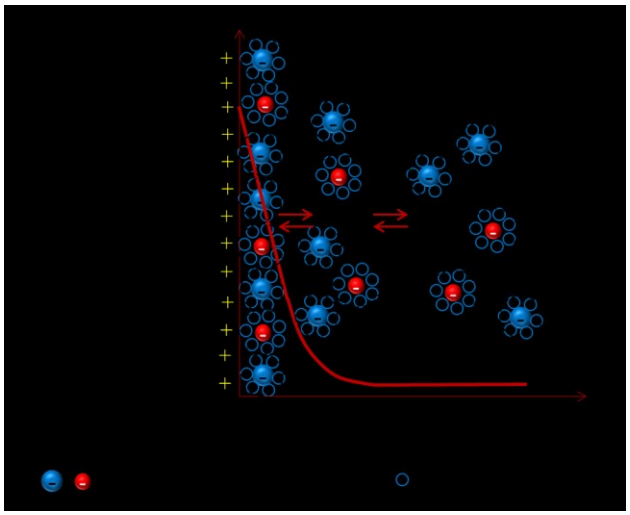

Figure 1. Scheme of CP^+ micellar triple-layer model, after (Lin and Jafvert, 2000).

When anions (A^{n-}) are added to the CPC solution, the binary ion exchange process on the micelles is as described by **eq 5**.

$$A^{n-} + nCl^-_{associated} \leftrightarrow nCl^- + A^{n-}_{associated} \quad (5)$$

where A^{n-} refers to free anions in the diffuse layer, with charge n; and the subscript "associated" designates anions associated with the micelles. When the system reaches equilibrium, the equilibrium constant (K_{eq}) is expressed by **eq 6**.

$$K_{eq} = \frac{\{A^{n-}\}_{associated}\{Cl^-\}^n_{dif}}{\{A^{n-}\}_{dif}\{Cl^-\}^n_{associated}} \quad (6)$$

where {i} refers to the activity of anions, and subscript "dif" represents the diffuse layer. The activity of ions in the diffuse layer can be calculated by the Boltzmann equation (**eq 7**).

$$\{A^{n-}\}_{dif} = \{A^{n-}\}_{aq} exp\frac{nF\psi}{RT} \quad (7)$$

where F represents Faraday's constant, ψ is the electrical potential at the Stern layer and diffuse layer boundary, R is the universal gas constant, and T is the absolute temperature. Combining and rearranging **eqs 6** and **7** yields the expression for K_{eq} shown in **eq 8**.

$$K_{eq} = \frac{\{A^{n-}\}_{associated}(\{Cl^-\}_{aq}\exp\left(\frac{F\psi}{RT}\right))^n}{\{Cl^-\}^n_{associated}\{A^{n-}\}_{aq}\exp\left(\frac{nF\psi}{RT}\right)} = \frac{\{A^{n-}\}_{associated}\{Cl^-\}^n_{aq}}{\{Cl^-\}^n_{associated}\{A^{n-}\}_{aq}} \quad (8)$$

However, the Stern layer is difficult to separate from the diffuse layer by membrane separation because the charge balance of the micellar solution must be maintained. In addition, the associated counterion fraction on the micelles is a function of numerous conditions such as counterion type, ionic strength, and temperature (Rathman and Scamehorn, 1984; Chen and

Jafvert, 2017). Therefore, the micellar concentration of ions (i.e., total counterion concentrations on micelles rejected by membrane, keeping charge balanced on the micelles) was substituted for the associated ion concentration to calculate the apparent equilibrium constant (**eq 9**), based on the assumption that the ratio of ions in the diffuse layer insignificantly influences the overall mass balance over a certain range of ionic strengths (Chen and Jafvert, 2017). Because this study focused on As (V) removal from fresh waters with low ionic strength, activity coefficients could be ignored when calculating the selectivity coefficients (K_{sel}, **eq 10**) used to characterize the affinity of a given anion for the micellar phase. The concentration of each anion (A_i^{n-}, i = 1 to ∞, including Cl^-) in the micellar phase ($[A_i^{n-}]_{mic}$, mole per mole of CP^+ monomer within micelles) was calculated using **eqs 11** and **12**.

$$K_{eq} \approx \frac{\{A^{n-}\}_{mic}\{Cl^-\}_{aq}^n}{\{Cl^-\}_{mic}^n\{A^{n-}\}_{aq}} \quad (9)$$

$$K_{sel} = \frac{\gamma_{A_{aq}^{n-}}\gamma_{Cl_{mic}^-}^n}{\gamma_{A_{mic}^{n-}}\gamma_{Cl_{aq}^-}^n} K_{eq} = \frac{[A^{n-}]_{mic}[Cl^-]_{aq}^n}{[A^{n-}]_{aq}[Cl^-]_{mic}^n} \quad (10)$$

$$[A_i^{n-}]_{mic} = \frac{[A_i^{n-}]_{total} - [A_i^{n-}]_{aq}}{M} \quad (11)$$

$$M = [CPC] - CMC = \sum_i n\,([A_i^{n-}]_{total} - [A_i^{n-}]_{aq}) \quad (12)$$

where M is the concentration of surfactant monomers within micelles, i.e., the concentration of exchange sites on the micelles (mol L^{-1}). To maintain a mass balance, M must also equal the total equivalent micellar anion concentration (**eq 12**).

2.5 Modeling As (V) ion exchange in a competitive environment

The simplified model used in this study, based on mass balances, mass reaction (selectivity coefficients), and the distribution of ionic species between the aqueous phase and a pseudo-

198 solid micellar phase, was developed and verified in a previous study (Chen and Jafvert, 2017). In
199 this study, the CMC was taken into consideration in modifying the mass balance equations and
200 calculating the phase distribution of As (V) and other anions in mixtures of anions. The model
201 equations are shown in **Table 1**. The initial anion concentrations in each water sample were
202 determined prior to adding a known concentration of CPC into the water. The pH of the sample
203 was measured after CPC addition, and then adjusted to the desired value using HCl or NaOH, as
204 appropriate. The total chloride concentration was then calculated as the sum of the initial
205 sample concentration, plus any chloride added with the CPC and for pH adjustment. Selectivity
206 coefficients for binding of anions to micelles were obtained using binary ion exchange
207 experiments. Unknown values were the concentrations of anions in the aqueous and micellar
208 phases. The equations of the model were solved using "Solver" in Microsoft Excel to iteratively
209 minimize the sum of squared errors by adjusting initially guessed values of the unknowns.

210 **Table 1.** Model equations for calculating concentrations of As (V) in micellar solutions

Mass balance equations	$[A_i^{n-}]_{total} = [A_i^{n-}]_{aq} + [A_i^{n-}]_{mic} * M$ †,‡
	$[As]_{total} = [H_2AsO_4^-]_{aq} + [H_2AsO_4^-]_{mic} * M + [\mathrm{H}AsO_4^{2-}]_{aq} + [\mathrm{H}AsO_4^{2-}]_{mic} * M$
	$\sum_i n[A_i^{n-}]_{mic} = 1$
CMC calculation	$M = [CPC]_{total} - CMC$
	$lnCMC = aln[Q]_{aq} + b$ ††
	$[Q]_{aq} = \sum_i [A_i^{n-}]_{aq}$

Selectivity coefficients	$K_{sel}{}_{Cl^-}^{A_i^{n-}} = \frac{[Cl^-]_{aq}^n [A_i^{n-}]_{mic}}{[Cl^-]_{mic}^n [A_i^{n-}]_{aq}}$
As species dependence on pH[§]	$pH = -\log[H^+]$ $K_a = \frac{[H^+][HASO_4^{2-}]}{[H_2AsO_4^-]} = 10^{-6.98}$

[†] A_i refers to each anion *i* in the system, including Cl^-, $H_2AsO_4^-$, $HAsO_4^{2-}$, NO_3^-, HCO_3^-, and SO_4^{2-} in this study, while mass balance equations for As are listed separately.

[‡] $[Cl^-]_{total} = [Cl^-]_{initial} + [Cl^-]_{CPC} + [Cl^-]_{HCl}$

[††] a = -0.641, b = -11.551 (Rathman and Scamehorn, 1984)

[§] The activity coefficient was ignored for calculation of pH and K_a.

(Unknowns in equations: $[A_i^{n-}]_{aq}, [A_i^{n-}]_{mic}, M, CMC, [Q]_{aq}, [H^+]$)

3. Results and discussion

3.1 As (V) removal by MEUF as a function of CPC concentration

Removal of As (V) by MEUF was first investigated by varying the concentration of CPC added. **Figure 2a** shows the results for MEUF of a 0.1 mM solution of As (V) at pH 7.5 for CPC concentrations ranging from 0 to 12 mM. When 5 mM CPC was added without any additional NaCl (giving a Cl^- concentration of 5 mM due to ions accompanying the CPC), 90% (*R* = 0.9) of the As (V) was rejected. Rejection increased to 94% when the CPC concentration was increased to 8 mM, again with no NaCl addition. These results are comparable to those of Iqbal *et al*.(2007), who reported 85% removal of As at 5 mM CPC and 94 - 96% removal at 10 mM CPC. Gecol *et al*.(2004) also observed high removal (90.9% - 100%) of As by MEUF (5 kDa and 10 kDa) with 10 mM CPC at pH 5.5 and 8.0. However, as shown in **Figure 2a**, a high concentration of competing anions, 5 mM Cl^- (added as NaCl), inhibited removal of As (V) by MEUF. Rejection of As (V)

dropped from 90 to 73% at 5 mM CPC, and from 94 to 89% with 10 mM CPC. Cationic surfactant micelles are in essence acting as nano-sized ion exchangers and, as expected, higher concentration of competing ions reduce binding of target ions.

Figure 2b shows the CPC concentrations in the permeate following UF separation. For the solution containing only 0.1 mM As (V) and CPC, almost all of the CPC passed the UF membrane at CPC concentrations under 0.6 mM. At CPC concentrations above 2 mM, the CPC concentration in the permeate remained about 0.92 mM, indicating that micelles large enough to be retained had formed. Free surfactant monomers and micelles exist in equilibrium when surfactant concentration exceeds the CMC (Chen and Szostak, 2004). Typical CPC micelles cannot pass a 10 kDa membrane (see **Figure 5S in the supporting information** for the particle size distribution of a 5 mM CPC suspension), but CPC monomers are small enough to pass through such membranes. When 5 mM NaCl was added to the 0.1 mM As (V) solution, much less CPC passed through the membrane – only 0.32 mM (average value) for CPC concentrations above 2 mM as shown in **Figure 2b** – because the CMC decreased as ionic strength increased. According to the CMC calculation equation in Table 1 (Rathman and Scamehorn, 1984), the CMC of CPC at 5 mM NaCl is calculated as 0.29 mM, close to the experimental values, which ranged from 0.27 mM to 0.33 mM.

Figure 2c shows As (V) removal and CPC retention at low CPC concentrations, above and below the CMC, the concentration at which micelle formation is significant. In the absence of CPC and competing anions, 16-38% (average = 24%, R = 0.24) of the As (V) was removed by membrane adsorption. As the CPC concentration was increased, rejection of As (V) increased to above 40% with 0.2 mM CPC, decreased to 23% with 0.6 mM CPC, then increased sharply as the CPC concentration increased beyond 0.6 mM CPC. Below 0.6 mM CPC, there was almost no CPC

rejected by the membrane because no micelles had formed. The small and varying removals of As (V) observed were presumably caused by a complex adsorption process, including adsorption of As (V) and CPC monomer onto the membrane, as well as desorption of As (V) and complexes of As (V) and CP^+ adsorbed onto the membrane, due to increased competition from Cl^- as the CPC concentration increased. A previous study reported anion rejection by a UF membrane was enhanced by surfactant concentrations much lower than the CMC, because of the adsorption of surfactant monomers on the membrane (Morel et al., 1997). As shown in **Figure 2c**, adding 5 mM of Cl^- ions reduced As (V) removal in the absence of CPC, presumably by competing for adsorption sites on the UF membrane, but significantly increased As (V) removal at CPC concentrations greater than 0.4 mM by causing increased formation and retention of micelles.

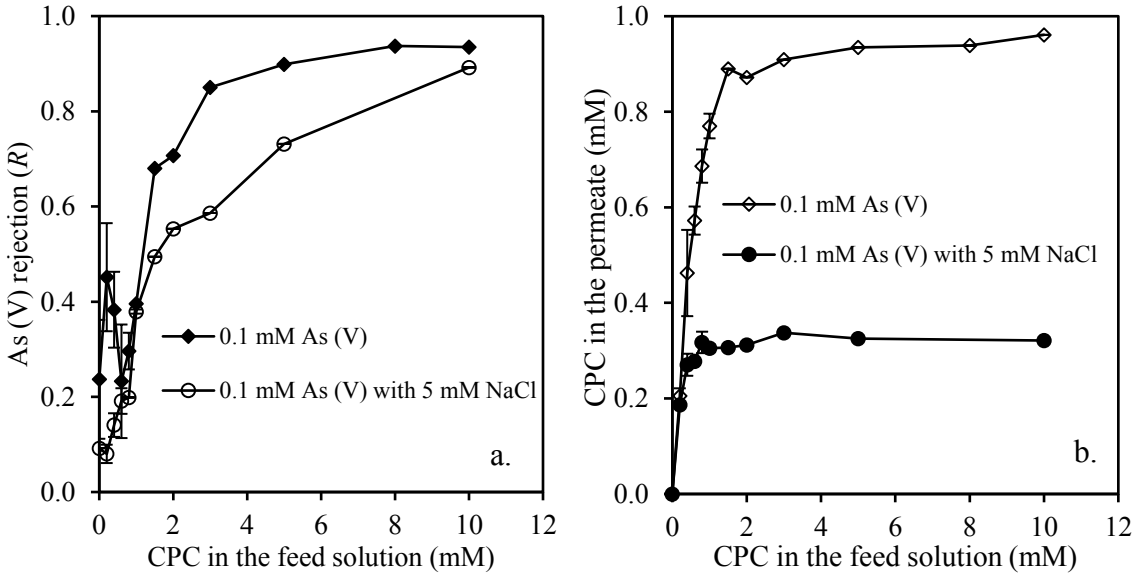

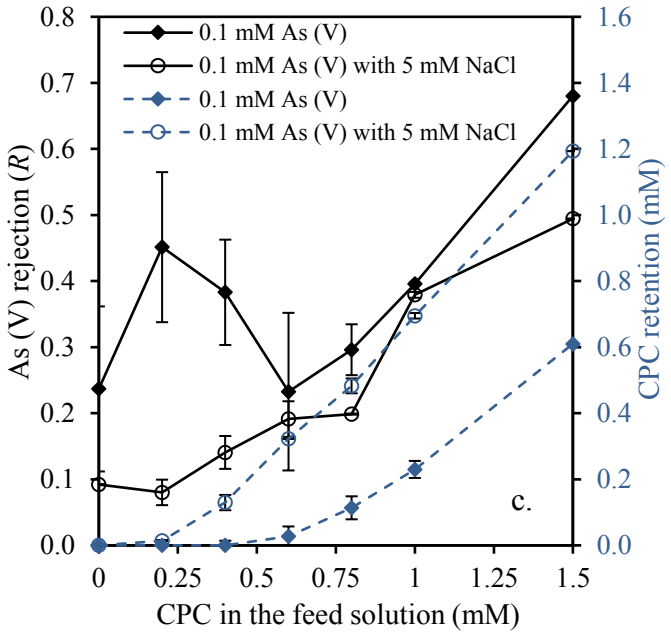

263

264 **Figure 2.** MEUF performance as a function of CPC concentration: (a) rejection of As (V) with and
265 without addition of 5 mM Cl^-; (b) CPC concentrations in the permeate; and (c) rejection of As (V)
266 and retention of CPC.

267 **3.2 Selectivity coefficients for binding of As (V) to CP^+ micelles**

268 **Equation 10**, which defines selectivity coefficients for binding of anions by micelles in binary
269 systems, can be rearranged to express the ratio of ions in the micellar phase as a linear function
270 of the ratio in the aqueous phase (**eq 13**), and the linear regression of this equation for a given
271 set of experimental conditions can be used to calculate the value of K_{sel} (Chen et al., 2017; Chen
272 and Jafvert, 2018; Chen et al., 2018).

273 $$\frac{[A^{n-}]_{mic}}{[Cl^-]^n_{mic}} = K_{sel}\frac{[A^{n-}]_{aq}}{[Cl^-]^n_{aq}} \qquad (13)$$

274 **Figure 3a** shows the ratio of $[H_2AsO_4^-]$ to $[Cl^-]$ in the CP^+ micellar phase regressed against
275 their ratio in the aqueous phase according to **eq 13**. The slope of the regression plot represents

the selectivity coefficient for $H_2AsO_4^-$, which was determined to be 0.55 (unitless). The dashed line in **Figure 3a** represents a selectivity of 1 (i.e., no preference for either ion). A higher slope indicates a greater affinity for the CP^+ micelles. Therefore, CP^+ has a lower affinity for $H_2AsO_4^-$ than for Cl^-. Previous studies have reported the selectivity coefficients for HCO_3^- and NO_3^- for CP^+, relative to Cl^-, as 0.60 and 2.73 (unitless), respectively (Chen and Jafvert, 2017). Thus, the affinity order for binding of these monovalent anions, commonly present in natural waters, to CP^+ micelles is $NO_3^- > Cl^- > HCO_3^- > H_2AsO_4^-$. The selectivity coefficient (affinity) is directly related to the Gibb's free energy change for the ion exchange reaction. For outer-sphere ionic complexation, the free energy change is a function of the ionic radius and ionic charges (Pauley, 1954; Sodaye et al., 2007). For ions with same valence, the difference of their affinities to the micelles (or other ion exchange materials) is primarily caused by the ionic radius (Chen and Jafvert, 2018; Chen et al., 2018), because an ion with smaller ionic radius will hydrated with more water molecules, which decreases the attractive force for the micellar surface.

Figure 3b shows the ratio of $[HAsO_4^{2-}]$ to the square of $[Cl^-]$ in the CP^+ micellar phase regressed against the same ratio in the aqueous phase. (As shown in **eq 10**, the Cl^- concentration is squared when exchanging a divalent ion for a monovalent ion.) The selectivity coefficient for binding of $HAsO_4^{2-}$ by CP^+ micelles, with respect to Cl^-, is 0.047 mol L^{-1} based on the slope of the regression plots, which is lower than reported selectivity coefficient for binding of SO_4^{2-} by CP^+ micelles (0.0706 mol L^{-1}) (Chen and Jafvert, 2017). Note that, for divalent anions, the selectivity coefficient has units of mol L^{-1} because of the squared values in the regression equation. Therefore the values of the selectivity coefficients for divalent anions cannot be directly compared with those for monovalent anions. The affinity of CPC for divalent *versus* monovalent anions is discussed in the following section.

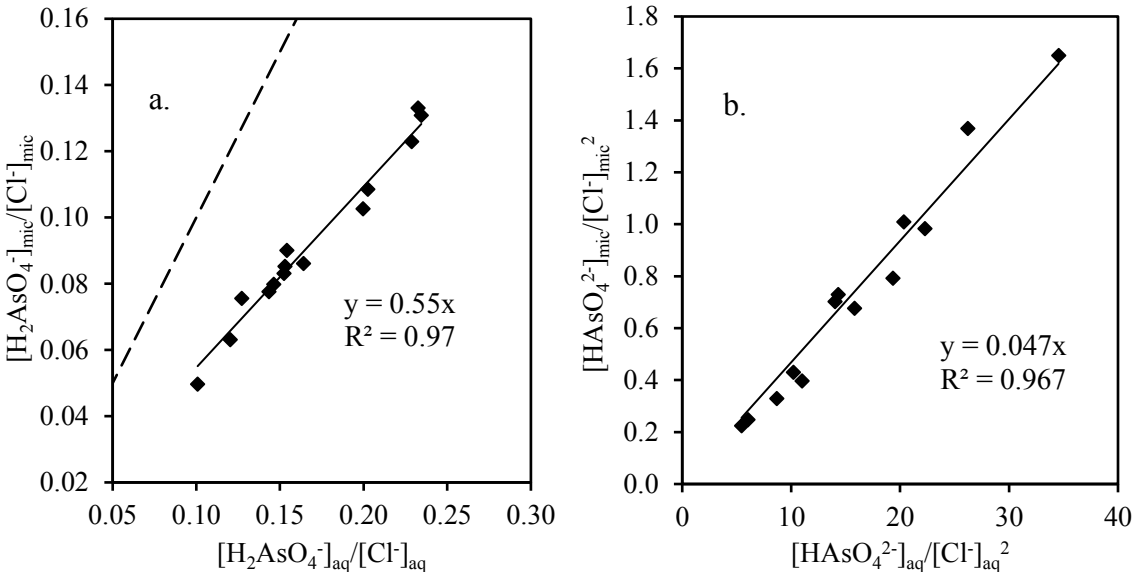

299

300 **Figure 3.** Regression plots for As (V) selectivity by CP^+ micelles relative to Cl^-: (a) for $H_2AsO_4^-$ (pH
301 = 4.5); (b) for $HAsO_4^{2-}$ (pH = 9.0). The initial total As (V) and CPC concentrations were 1 mM and
302 5 - 10 mM, respectively.

303 **3.3 Distribution of As (V) in the aqueous and micellar phases**

304 "Ion exchange isotherms" can be used for describing ion distribution in the aqueous and
305 micellar phases, and they are especially useful for comparing removals of monovalent and
306 divalent ions on a single graph. They are typically normalized by expressing the concentrations
307 in each phase as equivalent fractions, which can be calculated using **eqs 14-16**.

308 $$C = \sum_i n[A_i^{n-}]_{aq} \quad (14)$$

309 $$x_i = n[A_i^{n-}]_{aq}/C \quad (15)$$

310 $$y_i = n[A_i^{n-}]_{mic} \quad (16)$$

where, C is the total normality of the anions in solution (eq L^{-1}); and x_i and y_i refer to the equivalent fraction of anion A_i in the aqueous and micellar phases, respectively. $\sum x_i = 1$ and $\sum y_i = 1$.

In a binary system containing only $H_2AsO_4^-$ and Cl^-, the equivalent fraction of $H_2AsO_4^-$ in the CP^+ micellar phase (y) can be expressed as a function of the equivalent fraction of $H_2AsO_4^-$ (x) in the aqueous phase, as shown in **eq 17** (Chen and Jafvert, 2017).

$$y = \frac{K_{sel}x}{1-x+K_{sel}x} \quad (17)$$

According to **eq 17**, the phase distribution of the monovalent anion $H_2AsO_4^-$ in a binary system depends only on K_{sel}. Therefore, at relatively low ionic strength, where the K_{sel} is constant, the concentrations of these monovalent anions do not affect the distribution of $H_2AsO_4^-$ in a mono/mono-anion exchange system. K_{sel} for binding of $H_2AsO_4^-$ relative to Cl^- is less than 1, so the isotherm for $H_2AsO_4^-$ lies below the line of $y = x$ shown in **Figure 4**. This illustrates once again that the CP^+ micellar phase has less affinity for $H_2AsO_4^-$ than for Cl^-.

For binding of ions by micelles in a binary system, the phase distribution of a target divalent anion being exchanged for a monovalent ion can be expressed using **eq 18** (Lee et al., 2007).

$$y = 1 - ((1 + \frac{4K_{sel}x}{C(1-x)^2})^{0.5} - 1)/(\frac{2K_{sel}x}{C(1-x)^2}) \quad (18)$$

Figure 4 shows the model-calculated phase distributions of 1 mM As (V) at varying pH values using **equations 17** and **18**, including one set of calculations with 5 mM additional Cl^- ions added in the form of NaCl. The open symbols show the previously described experimental results (from **Figure 3**) compared to these calculations, while the filled symbols show experimental results for As (V) at pH 6 and with 5 mM NaCl. The isotherm for binding of $H_2AsO_4^{2-}$ by CPC, in a binary

system containing only 1 mM $HAsO_4^{2-}$, lies well above the line of $y = x$, indicating that the CP^+ micelles have a much higher affinity for the divalent $HAsO_4^{2-}$ anions than for the monovalent $H_2AsO_4^-$ or Cl^- ions.

It should be noted that, unlike the phase distribution of monovalent anions, the phase distribution of divalent ions, including $HAsO_4^{2-}$ is related to K_{sel}/C. Therefore, increasing the concentration of competing ions (i.e., a higher total normality of anions in the aqueous phase, C) leads to a lower fraction of target ions in the micellar phase. Put another way, increasing the number of competing anions causes the distribution of As to shift towards the aqueous phase, moving the isotherm closer to the line of $y = x$. Ignoring other effects, if the concentration of competing ions increases sufficiently, the isotherm can even drop below the line of $y = x$, indicating that As preferentially remains in the aqueous phase. With 5 mM NaCl added to solution, the $HAsO_4^{2-}$ isotherm in **Figure 4** lies closer to the $y = x$ line, i.e., the fraction of $HAsO_4^{2-}$ in the micellar phase is lower for any given aqueous phase equivalent fraction when more ions are present in solution. Take x = 0.1 for example; when the aqueous phase fraction is 0.1, the micellar phase fraction of $HAsO_4^{2-}$ with only CPC and 1 mM As in the solution is around 0.5, but the micellar phase fraction is only 0.35 with 5 mM Cl^- added. As described in **eq 18**, for a divalent-monovalent system, the micellar fraction of the divalent ion depends on C, the total normality. Thus, any increase in the total number of ions in the aqueous phase will reduce the divalent ion preference for the micellar phase. This has also been observed with SO_4^{2-} and HPO_4^{2-} in a previous study (Chen and Jafvert, 2017).

At pH 6, 85% of As (V) in the aqueous phase is $H_2AsO_4^-$ and the other 15% is $HAsO_4^{2-}$ (as illustrated in the pC-pH diagram for As (V) shown in **Figure 1S** in the **Supporting Information**). Therefore, the system at pH 6 is a ternary system (consisting of the two arsenic species plus Cl^-),

355 so the phase distributions of $H_3AsO_4^-$ and $H_2AsO_4^{2-}$ cannot be modeled using **eq 17** or **18**, which
356 apply only to binary systems. The model shown in **Table 1**, coupled with **eqs 1-3** to quantify As
357 (V) speciation as a function of pH, was used to determine the phase distribution line for 1 mM
358 As (V) at pH 6. This adjusted model corresponds well to the experimental data (**Figure 4**). The
359 isotherm for As (V) at pH 6 is located between the line of $H_2AsO_4^-$ (monovalent As (V), lower
360 affinity) and $HAsO_4^{2-}$ (divalent As (V), higher affinity).

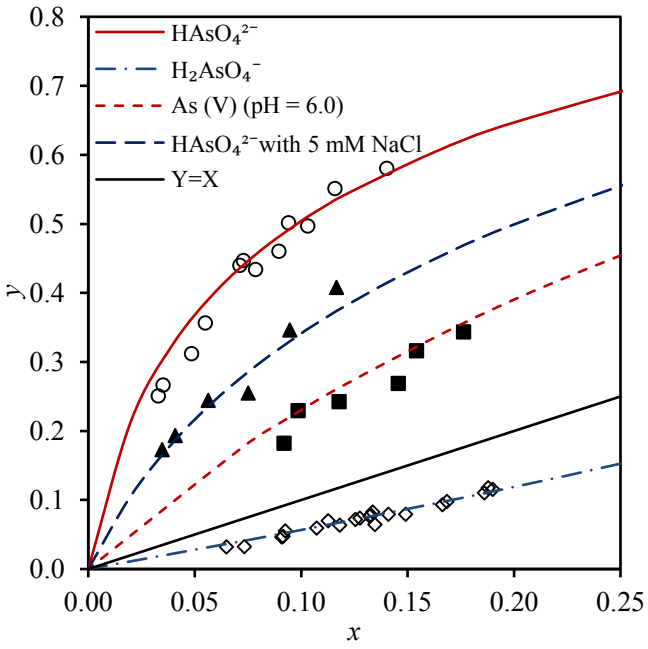

361

362 **Figure 4.** Equivalent fraction of As (V) in the CP^+ micellar phase (y) *versus* the equivalent fraction
363 of As (V) in the aqueous phase (x), with Cl^- as the co-ion, as a function of pH and NaCl addition at
364 1 mM initial As (V). Lines illustrate model calculations; symbols show experimental data.

365 **3.4 The effect of pH and competing anions on As (V) removal**

366 Removal of 0.1 mM As (V) using 5 mM CPC over a range of pH values, with 5 mM NaCl
367 added, is shown in **Figure 5a**. Rejection of As (V) increased from 0.39 to 0.89 as the pH
368 increased from 5.0 to 8.2, with good agreement between the experimental results and model-

calculated values. Higher pH leads to a higher As removal because As (V) is increasingly present as a divalent anion with a higher affinity for CP^+ micelles. These results are consistent with previous studies of As removal using CPC micelles (Gecol et al., 2004) and cationic polymers (Molinari and Argurio, 2017), both of which observed better removal as pH became more basic.

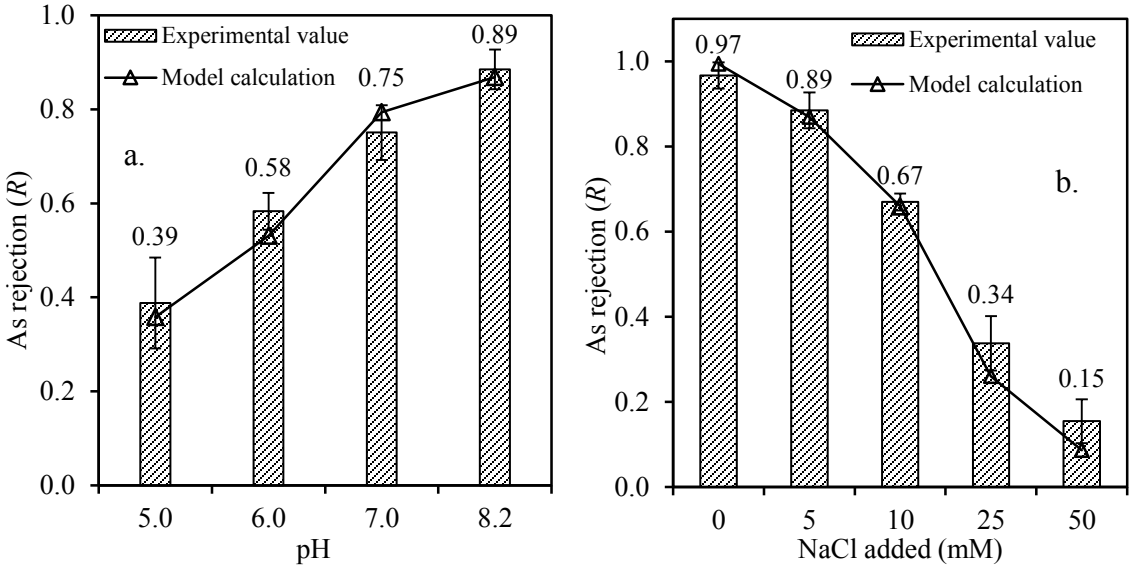

Figure 5. Measured and calculated As (V) removal by MEUF (a) at different pH values in a system containing 0.1 mM As (V), 5 mM CPC, and 5 mM NaCl; (b) as a function of the concentration of added chloride. (The error bars represent standard deviations of repeated experiments.)

NaCl was added into water samples at concentrations varying from 0 to 50 mM to investigate the effect of increasing concentrations of a competing anion (Cl^-) on As (V) removal by MEUF. **Figure 5b** shows the results obtained for a 0.1 mM As (V) solution to which 5 mM CPC was added at pH 8.2. Rejection of As (V) decreased from 0.97 to 0.15 as the concentration of NaCl in the solution increased from 0 to 50 mM. As the fraction of Cl^- in the aqueous phase increased, the fraction of Cl^- in the micellar phase also increased, while the fraction of As (V) in the micellar phase decreased, as expected. Similar decreases in As removal resulting from

384 competing anions have were observed in previous studies (Ergican et al., 2005; Iqbal et al.,
385 2007).

386 The experimentally measured removals of As (V) were close to model-calculated values
387 based on K_{sel} when the concentration of Cl^- ranged from 0 to 10 mM. However, the experimental
388 removals were substantially higher than the calculated ones at Cl^- concentrations of 25 and 50
389 mM (**Figure 5b**). This may be because the true value of K_{sel} for As increased at a higher ionic
390 strength. From **eq 10**, K_{sel} was considered equal to K_{eq} and relatively constant over a range of
391 low ionic strengths, but this assumption grows less accurate as ionic strength increases to the
392 point where the activity coefficients are significantly different from 1. Kim and Benjamin (Kim
393 and Benjamin, 2004) observed an increase in sulfate/nitrate selectivity for an ion exchange resin
394 as ionic strength increased. For better accuracy, the model should be adjusted as ionic strength
395 increases.

396 In addition, the simplified model uses $[A^{n-}]_{mic}$ as a surrogate for $[A^{n-}]_{associated}$ to calculate K_{sel}.
397 However, $[A^{n-}]_{mic}$ includes both anions in the Stern layer (the 'true' $[A^{n-}]_{associated}$) and anions in the
398 diffuse layer ($[A^{n-}]_{dif}$). As the ionic strength increases, the fraction of ions on the Stern layer also
399 increases (Lin and Jafvert, 2000). As a result $[A^{n-}]_{associated}$ and $[A^{n-}]_{mic}$ approach the same value,
400 and the apparent selectivity coefficient (K_{sel}) for As increases, becoming closer to the real K_{eq}. A
401 similar trend of increasing apparent selectivity of micelles for I^- relative to Br^- was also reported
402 as a function of increasing ionic strength (Warr, 1997).

403 **3.5 Model predictions of As (V) removal from mixtures of anions**

404 Arsenic removal from mixtures of anions by MEUF was assessed in both artificial waters and
405 a surface water sample spiked with As (V). Artificial water samples contained As (V) at 0.1 mM,
406 Cl^-, NO_3^- and SO_4^{2-} each at 1 mM concentration, and HCO_3^- at 5 mM. All anions were added to

deionized water as sodium salts, resulting in a final pH of 8.2. **Figure 6** shows the measured As (V) rejection by MEUF, as well as the removal expected based on model calculations. Arsenic (V) removal increased from 38% to 91% as the concentration of CPC increased from 3 mM to 25 mM. (Arsenic removal was 3% in the absence of CPC addition.) Predicted and experimental As removals for this system were not significantly different at 95% confidence (p = 0.108), based on a pair-sample t-Test. **Table 2** shows the predicted and measured concentrations of all anions in the permeate when 25 mM CPC was added to the artificial water sample. Increasing the concentration of sulfate to 5 mM resulted in a decrease in As (V) removal from 90% to 69% due to enhanced competition from divalent sulfate ions. In addition, the concentration of CPC in the permeate decreased due to the higher ionic strength (lower CMC). Similar effects of anion competition have been observed in published studies. For example, Ergican *et al*. (2005) investigated the effect of co-occurring inorganic solutes on arsenic removal from well water by MEUF and found that As removal decreased as the sulfate concentration increased from 28 to 400 ppm.

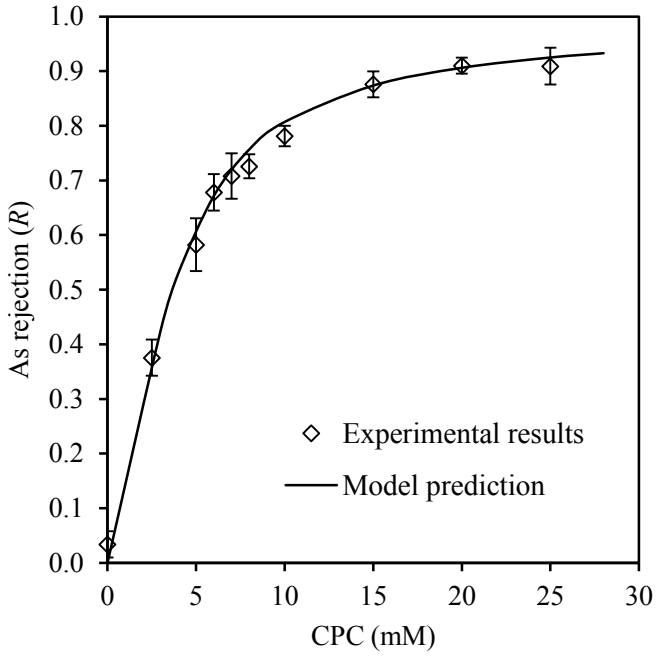

Figure 6. As (V) removal by CPC from artificial water samples. (The error bars represent standard deviations of repeated experiments.)

Table 2. Predicted and measured concentrations of anions in the MEUF permeate

Test Condition	Sample	Concentration (mM)						As Rejection
		SO_4^{2-}	NO_3^-	HCO_3^-	Cl^-	As (V)	CMC	
25 mM CPC 1 mM SO_4^{2-}	Meas. initial	1.118	1.074	5.050	24.990	0.105		
	Predicted Perm.	0.061	0.139	2.026	7.453	0.009	0.187	0.92
	Measured Perm.	0.060	0.125	2.193	7.900	0.011	0.213	0.90
25 mM CPC 5 mM SO_4^{2-}	Meas. initial	5.204	1.084	4.720	25.583	0.102		
	Predicted Perm.	1.089	0.262	2.780	11.860	0.029	0.130	0.71
	Measured Perm.	0.955	0.207	3.073	12.304	0.032	0.136	0.69

Figure 7a shows the removal of As (V), SO_4^{2-}, and HCO_3^- by MEUF, from the spiked Kansas River water samples, at CPC concentrations from 5 to 20 mM. The removal of As from the spiked Kansas River water samples was 5-10% lower than that from the artificial waters at the same concentrations of CPC, due to stronger competition from other anions. As expected, SO_4^{2-} was strongly rejected (91% at 20 mM CPC) due to its strong affinity for CP^+ micelles, and HCO_3^- was the least rejected because of its low affinity for CP^+ micelles. Because the pH of the water samples was above 8, most of As (V) was present as $HAsO_4^{2-}$, which has a relatively high affinity for CP^+ micelles. Removal of As (V) increased from 0.50 to 0.84 as the concentration of CPC increased from 5 mM to 20 mM.

435 **Figure 7b** compares the measured concentrations of anions and CP^+ monomers in the MEUF
436 permeate with the model-calculated values. The added CPC concentration ranged from 5 to 20
437 mM. There was good agreement between measured and model-calculated values for all
438 constituents except for Cl^-, for which the measured Cl^- concentrations were higher than model-
439 calculated concentrations. (The average error between measured and model-calculated
440 concentrations of Cl^- is only 6.2%, and all agree to within 10%.)

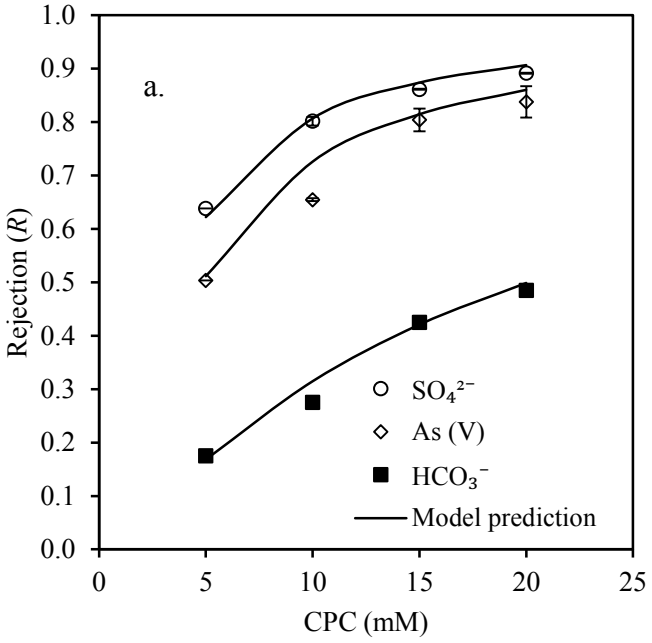

441

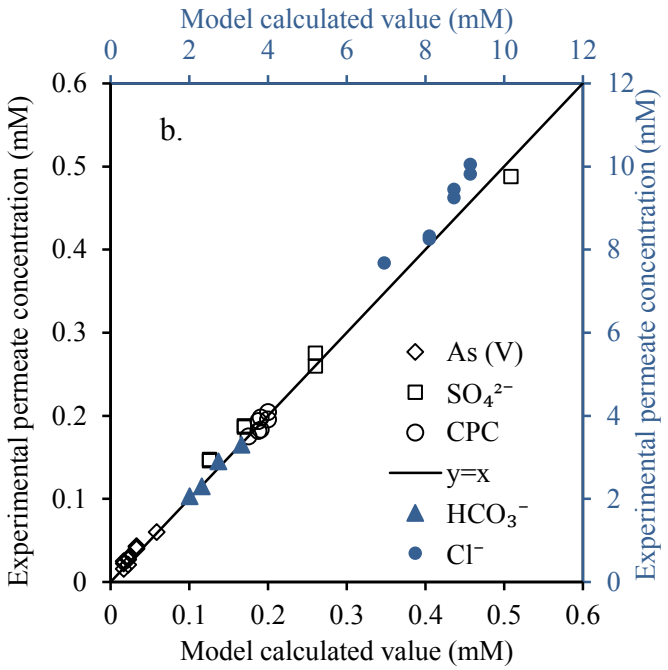

442

443 **Figure 7**. Measured and model-predicted results of the spiked Kansas River water samples. (a)
444 rejection of anions from Kansas River water samples spiked with 0.12 mM As (V); (b)
445 relationship between measured and model-calculated concentrations of anions and CPC in the
446 permeate (with upper and right axes for Cl^- and HCO_3^- and left and lower axes for As (V), SO_4^{2-}
447 and CPC).

448 **4. Summary and Conclusions**

449 This study evaluated and modeled As (V) removal, from both synthetic solutions and spiked
450 samples of natural water, by micellar enhanced ultrafiltration (MEUF), using cetylpyridinium
451 chloride (CPC) to form the micelles. Monovalent arsenate was poorly removed, but greater than
452 90% removal of divalent arsenate (the predominant form at pH values >7) was achieved using
453 ≥5 mM CPC in the absence of competing anions. The selectivity coefficient for $H_2AsO_4^-$ uptake by
454 CP^+ micelles was determined to be 0.55 (unitless) with respect to Cl^-, and the affinity order for
455 monovalent anions was $NO_3^- > Cl^- > HCO_3^- > H_2AsO_4^-$. The selectivity coefficient for $HAsO_4^{2-}$ was

0.047 mol L^{-1}, lower than that for SO_4^{2-}. Competing anions decreased removal of As (V), as expected. A simplified model based on mass balances across UF membranes, selectivity coefficients determined from test results on binary systems, and As speciation as a function of pH was used to predict As (V) removal by MEUF. The predicted values were in good agreement with experiment results for both synthetic solutions and samples of natural river water containing mixtures of anions. These results suggest that As removal will be more limited in waters with high concentrations of competing anions. Adjustments to the model may be considered in future research to predict As (V) removal from wastewaters or other waters with high ionic strength.

Supporting Information

Supporting information available includes a pC-pH diagram and a predominance area diagram for As (V); a UV absorbance spectrum and a standard curve for determining CPC concentrations; the particle size distribution of CPC micelles; and anionic composition of Kansas River water sample.

Conflicts of interest

There are no conflicts to declare.

Acknowledgement

This study was financially supported by the National Science Foundation EPSCoR Track Research Infrastructure Improvement Program: Track-2 Focused EPSCoR Collaboration award (OIA-

1632892). The authors also would like to acknowledge and thank support from the China Scholarship Council (CSC, NO. 201306090107) to M. Chen.

References

APHA, AWWA, WEF, 2012. Standard methods for the examination of water and wastewater, 22nd Edition. American Public Health Association, American Water Works Association, Water Environment Federation, Washington, DC, USA.

Beolchini, F., Pagnanelli, F., De Michelis, I., Veglio, F., 2006. Micellar enhanced ultrafiltration for arsenic (V) removal: effect of main operating conditions and dynamic modelling. Environ. Sci. Technol. 40, 2746-2752.

Beolchini, F., Pagnanelli, F., De Michelis, I., Veglio, F., 2007. Treatment of concentrated arsenic (V) solutions by micellar enhanced ultrafiltration with high molecular weight cut-off membrane. J. Hazard. Mater. 148, 116-121.

Bissen, M., Frimmel, F.H., 2003. Arsenic—a review. Part II: oxidation of arsenic and its removal in water treatment. CLEAN–Soil, Air, Water 31, 97-107.

Bräuner, E.V., Nordsborg, R.B., Andersen, Z.J., Tjønneland, A., Loft, S., Raaschou-Nielsen, O., 2014. Long-term exposure to low-level arsenic in drinking water and diabetes incidence: a prospective study of the diet, cancer and health cohort. Environ. Health Perspect. 122, 1059-1065.

Chen, I.A., Szostak, J.W., 2004. A kinetic study of the growth of fatty acid vesicles. Biophys. J. 87, 988-998.

Chen, M., Jafvert, C.T., 2017. Anion exchange on cationic surfactant micelles, and a speciation model for estimating anion removal on micelles during ultrafiltration of water. Langmuir 33, 6540-6549.

Chen, M., Jafvert, C.T., 2018. Anion recovery from water by cross-linked cationic surfactant nanoparticles across dialysis membranes. Environ. Sci.: Nano. 5, 1350-1360.

Chen, M., Shafer-Peltier, K., Randtke, S.J., Peltier, E., 2018. Competitive association of cations with poly (sodium 4-styrenesulfonate)(PSS) and heavy metal removal from water by PSS-assisted ultrafiltration. Chem. Eng. J. 344, 155-164.

Chen, M., Wu, Y., Jafvert, C., 2017. Synthesis of Cross-linked Cationic Surfactant Nanoparticles for Removing Anions from Water. Environ. Sci.: Nano. 4, 1534-1543.

Chilvers, D., Peterson, P., 1987. Global cycling of arsenic. Lead, mercury, cadmium and arsenic in the environment. John Wiley & Sons Ltd., New York, NY, USA, pp. 279-301.

Cui, J., Jing, C., Che, D., Zhang, J., Duan, S., 2015. Groundwater arsenic removal by coagulation using ferric(III) sulfate and polyferric sulfate: A comparative and mechanistic study. J Environ. Sci. 32, 42-53.

Cullen, W.R., Reimer, K.J., 1989. Arsenic speciation in the environment. Chem. Rev. 89, 713-764.

514 Dodd, M.C., Vu, N.D., Ammann, A., Le, V.C., Kissner, R., Pham, H.V., Cao, T.H., Berg, M., von
515 Gunten, U., 2006. Kinetics and mechanistic aspects of As (III) oxidation by aqueous
516 chlorine, chloramines, and ozone: relevance to drinking water treatment. Environ. Sci.
517 Technol. 40, 3285-3292.

518 Dominguez-Ramos, A., Chavan, K., García, V.n., Jimeno, G., Albo, J., Marathe, K.V., Yadav, G.D.,
519 Irabien, A., 2014. Arsenic removal from natural waters by adsorption or ion exchange: an
520 environmental sustainability assessment. Ind. Eng. Chem. Res. 53, 18920-18927.

521 Elton, J., Hristovski, K., Westerhoff, P., 2013. Titanium dioxide-based hybrid ion-exchange media
522 for simultaneous removal of arsenic and nitrate. in: Satinder Ahuja, K.H. (Ed.). Novel
523 Solutions to Water Pollution. American Chemical Society, pp. 223-236.

524 EPA, 2000. Technologies and costs for removal of arsenic from drinking water. EPA- 815-R-00-
525 028, EPA Office of Water, Washington, DC, USA.

526 EPA, 2001. National Primary Drinking Water Regulations: Arsenic and Clarifications to
527 Compliance and New Source Contaminants Monitoring. Federal Register 66, 69-76.

528 Ergican, E., Gecol, H., 2008. Nonlinear two-phase equilibrium model for the binding of arsenic
529 anions to cationic micelles. J. Membr. Sci. 325, 69-80.

530 Ergican, E., Gecol, H., Fuchs, A., 2005. The effect of co-occurring inorganic solutes on the
531 removal of arsenic (V) from water using cationic surfactant micelles and an ultrafiltration
532 membrane. Desalination 181, 9-26.

533 Garelick, H., Jones, H., Dybowska, A., Valsami-Jones, E., 2009. Arsenic pollution sources. Reviews
534 of Environmental Contamination. Springer, pp. 17-60.

535 Gecol, H., Ergican, E., Fuchs, A., 2004. Molecular level separation of arsenic (V) from water using
536 cationic surfactant micelles and ultrafiltration membrane. J. Membr. Sci. 241, 105-119.

537 Han, F.X., Kingery, W.L., Selim, H.M., Gerard, P.D., Cox, M.S., Oldham, J.L., 2004. Arsenic
538 solubility and distribution in poultry waste and long-term amended soil. Sci. Total Environ.
539 320, 51-61.

540 Hong, J., Zhu, Z., Lu, H., Qiu, Y., 2014. Synthesis and arsenic adsorption performances of ferric-
541 based layered double hydroxide with α-alanine intercalation. Chem. Eng. J. 252, 267-274.

542 Huang, J., Li, H., Zeng, G., Shi, L., Gu, Y., Shi, Y., Tang, B., Li, X., 2018. Removal of Cd (II) by MEUF-
543 FF with anionic-nonionic mixture at low concentration. Sep. Purif. Technol. 207, 199-205.

544 Huang, J., Yuan, F., Zeng, G., Li, X., Gu, Y., Shi, L., Liu, W., Shi, Y., 2017. Influence of pH on heavy
545 metal speciation and removal from wastewater using micellar-enhanced ultrafiltration.
546 Chemosphere 173, 199-206.

547 Iqbal, J., Kim, H.-J., Yang, J.-S., Baek, K., Yang, J.-W., 2007. Removal of arsenic from groundwater
548 by micellar-enhanced ultrafiltration (MEUF). Chemosphere 66, 970-976.

549 Jafari, A., Rezaee, R., Nasseri, S., Mahvi, A.H., Maleki, A., Safari, M., Shahmoradi, B., Daraei, H.,
550 2017. Application of micellar enhanced ultrafiltration (MEUF) for arsenic (v) removal from
551 aqueous solutions and process optimization. J. Dispersion Sci. Technol. 38, 1588-1593.

552 Jain, C., Ali, I., 2000. Arsenic: occurrence, toxicity and speciation techniques. Water Res. 34,
553 4304-4312.

554 Jiang, Y., Zeng, X., Fan, X., Chao, S., Zhu, M., Cao, H., 2015. Levels of arsenic pollution in daily
555 foodstuffs and soils and its associated human health risk in a town in Jiangsu Province,
556 China. Ecotoxicol. Environ. Saf. 122, 198-204.

557 Kim, J., Benjamin, M.M., 2004. Modeling a novel ion exchange process for arsenic and nitrate
558 removal. Water Res. 38, 2053-2062.

559 Lee, I.-H., Kuan, Y.-C., Chern, J.-M., 2007. Equilibrium and kinetics of heavy metal ion exchange. J.
560 Chin. Inst. Chem. Eng. 38, 71-84.

561 Lee, J., Yang, J.-S., Kim, H.-J., Baek, K., Yang, J.-W., 2005. Simultaneous removal of organic and
562 inorganic contaminants by micellar enhanced ultrafiltration with mixed surfactant.
563 Desalination 184, 395-407.

564 Lin, C.-C., Jafvert, C.T., 2000. A triple layer, planar coordinate model for describing counterion
565 association to micelles. Langmuir 16, 2450-2456.

566 Liu, X., Zhang, W., Hu, Y., Hu, E., Xie, X., Wang, L., Cheng, H., 2015. Arsenic pollution of
567 agricultural soils by concentrated animal feeding operations (CAFOs). Chemosphere 119,
568 273-281.

569 McArthur, J., Ghosal, U., Sikdar, P., Ball, J., 2016. Arsenic in groundwater: the deep late
570 Pleistocene aquifers of the Western Bengal Basin. Environ. Sci. Technol. 50, 3469-3476.

571 Molinari, R., Argurio, P., 2017. Arsenic removal from water by coupling photocatalysis and
572 complexation-ultrafiltration processes: A preliminary study. Water Res. 109, 327-336.

573 Mondal, P., Tran, A.T.K., Van der Bruggen, B., 2014. Removal of As(V) from simulated
574 groundwater using forward osmosis: Effect of competing and coexisting solutes.
575 Desalination 348, 33-38.

576 Morel, G., Ouazzani, N., Graciaa, A., Lachaise, J., 1997. Surfactant modified ultrafiltration for
577 nitrate ion removal. J. Membr. Sci. 134, 47-57.

578 Ning, R.Y., 2002. Arsenic removal by reverse osmosis. Desalination 143, 237-241.

579 Pauley, J., 1954. Prediction of cation-exchange equilibria. J. Am. Chem. Soc. 76, 1422-1425.

580 Rathman, J.F., Scamehorn, J.F., 1984. Counterion binding on mixed micelles. J. Phys. Chem. 88,
581 5807-5816.

582 Rivas, B.L., del Carmen Aguirre, M., Pereira, E., 2007. Cationic water‐soluble polymers with the
583 ability to remove arsenate through an ultrafiltration technique. J. Appl. Polym. Sci. 106,
584 89-94.

585 Savery, L.C., Wise, J.T.F., Wise, S.S., Falank, C., Gianios, C., Thompson, W.D., Perkins, C., Zheng, T.,
586 Zhu, C., Wise, J.P., 2014. Global assessment of arsenic pollution using sperm whales
587 (Physeter macrocephalus) as an emerging aquatic model organism. Comp. Biochem.
588 Physiol. C: Pharmacol. Toxicol. 163, 55-63.

589 Schwanck, F., Simões, J.C., Handley, M., Mayewski, P.A., Bernardo, R.T., Aquino, F.E., 2016.
590 Anomalously high arsenic concentration in a West Antarctic ice core and its relationship to
591 copper mining in Chile. Atmos. Environ. 125, 257-264.

592 Schwarze, M., 2017. Micellar-enhanced ultrafiltration (MEUF)–state of the art. Environ. Sci.:
593 Water Res. Technol. 3, 598-624.

Schwarze, M., Groß, M., Moritz, M., Buchner, G., Kapitzki, L., Chiappisi, L., Gradzielski, M., 2015. Micellar enhanced ultrafiltration (MEUF) of metal cations with oleylethoxycarboxylate. J. Membr. Sci. 478, 140-147.

Singh, R., Singh, S., Parihar, P., Singh, V.P., Prasad, S.M., 2015. Arsenic contamination, consequences and remediation techniques: a review. Ecotoxicol. Environ. Saf. 112, 247-270.

Sodaye, S., Suresh, G., Pandey, A., Goswami, A., 2007. Determination and theoretical evaluation of selectivity coefficients of monovalent anions in anion-exchange polymer inclusion membrane. Journal of membrane science 295, 108-113.

Sorg, T.J., Chen, A.S.C., Wang, L., 2014. Arsenic species in drinking water wells in the USA with high arsenic concentrations. Water Res. 48, 156-169.

Tang, X., Berner, Z., Nalcaci, O.O., Norra, S., 2015. Selective Separation and Preconcentration of Arsenite from Arsenic Enriched Natural Waters with Three Different Adsorbents. Sep. Sci. Technol. 50, 2112-2123.

Warr, G.G., 1997. Ion binding and the apparent selectivity coefficient for ion flotation. Langmuir 13, 1451-1456.

Welch, A.H., Westjohn, D., Helsel, D.R., Wanty, R.B., 2000. Arsenic in ground water of the United States: occurrence and geochemistry. Groundwater 38, 589-604.

Xie, J., Lai, L., Lin, L., Wu, D., Zhang, Z., Kong, H., 2015. Phosphate removal from water by a novel zeolite/lanthanum hydroxide hybrid material prepared from coal fly ash. J Environ. Sci. Heal. A. 50, 1298-1305.

Zhou, L., Zheng, W., Ji, Y., Zhang, J., Zeng, C., Zhang, Y., Wang, Q., Yang, X., 2013. Ferrous-activated persulfate oxidation of arsenic (III) and diuron in aquatic system. J. Hazard. Mater. 263, 422-430.